Computational study of the interactions between benzene and crystalline ice I_h: Ground and excited states

Divya Sharma,[a] W. M. C Sameera,[b,c] Stefan Andersson,[c,d] Gunnar Nyman,[c] and Martin J. Paterson*[a]

Abstract: Ground state geometries of benzene on crystalline ice cluster model surfaces (I_h) are investigated. It is found that the binding energies of benzene-bound ice complexes are sensitive to the dangling features of the binding sites. We used time-dependent DFT to study the UV spectroscopy of benzene, ice clusters, and benzene-ice complexes, employing the M06-2X functional. It is observed that the size of the ice cluster and the dangling features show minor effects on the UV spectral characteristics. Benzene–mediated electronic excitations of water towards longer wavelengths (above 170 nm) are noticed in benzene-bound ice clusters, where the cross-section of photon absorption water is negligible, in good agreement with recent experimental results (Thrower *et al*., *J. Vac. Sci. Technol. A*, 2008, **26**, 919-924). The intensities of peaks associated with water excitations in benzene-ice complexes are found to be higher than in isolated ice clusters. The $\pi \rightarrow \pi^*$ electronic transition of benzene in benzene-ice complexes undergoes a small red-shift compared to the isolated benzene molecule, and this holds for all benzene-bound ice complexes.

Introduction

Polycyclic aromatic hydrocarbons (PAHs) are one of the most important classes of carbon-bearing molecules.[1] They may account for up to 20 % of the carbon in our galaxy, and are now widely accepted as being ubiquitously present in many astrophysical environments.[2-6] They have also been proposed as possible carriers of both the diffuse interstellar bands (DIBs)[7] and the unidentified infrared bands (UIRs) observed in a wide range of environments. Moreover, PAHs are likely to exist as either a component of water-rich icy mantles that are accreted on dust grains under cold conditions ($T \leq 20$ K), or as a part of the carbonaceous component of the dust grain itself.[8, 9] Infrared (IR) observations on icy mantles have revealed H_2O as the most abundant molecule, along with some other species such as CO, CO_2, and CH_3OH.[2] Several experiments have been performed to obtain IR absorption spectra of PAH/H_2O ice mixtures.[10-12]

Chemical evolution of bulk ices during irradiation by UV light has been extensively studied.[13, 14] The photochemistry of H_2O ices containing PAHs upon irradiation by UV light has been studied experimentally using IR spectroscopy and mass spectrometry.[14-17] It has been observed that UV irradiation of water ice containing PAHs may play an important role in the formation of complex organic species such as alcohols, quinones and ethers including substituted PAH species.[14] Photon-stimulated desorption is an important process to account for the high gas phase abundances of water under astrophysically relevant conditions.[18, 19] Recently there has also been increased interest in the UV processing of laboratory models of interstellar ices.[20-29]

Benzene (Bz) has been detected in the proto-planetary nebula CRL 618,[30] and is chosen as a representative of complex PAH molecules within ice mantles, while crystalline water ice (I_h) structures are chosen to model water-dominated interstellar icy mantles. Under ambient conditions, hexagonal crystal ice is the dominant solid form of H_2O. Experimental and computational studies have been performed to understand the effect of temperature on the crystalline ice surfaces that leads to the proton ordering-disordering at the surface, which also affects the interactions between the ice crystal surface and different adsorbates.[31-33] Several previous experimental and computational studies in the literature discussed the patterns of dangling H (*d*-H) and dangling O (*d*-O) atoms at the basal ice surface.[31-35]

Numerous theoretical and experimental studies have been performed on ground state properties such as geometries, binding energies, and infrared (IR) spectra of water W_n clusters[36-46] and Bz-W_n complexes[47-50], with a detailed description of the non-covalent interactions, such as hydrogen bonding interactions prevailing in such systems.[41, 45-49, 51] Zwier and their co-workers have carried out extensive experimental studies on Bz-W_n complexes and IR data have been presented.[48, 52, 53] Experimental studies on the interaction between Bz and the surface of amorphous ice have shown that the Bz interacts with the ice surface as a proton acceptor, and a strong down-shift of the dangling-H band in the IR spectra of the ice is observed.[54] IR spectral characteristics of the ice-benzene system depend on the shape and position of the dangling-H band, which in turn depends on the temperature.

The interaction of Bz with amorphous solid water adsorbed on polycrystalline Ag has been studied experimentally.[55] Detailed computational studies of Bz-W_n (n = 1-10) complexes using DFT have shown the presence of nonconventional H-bonding interactions such as O-H$\cdots\pi$ interactions in all these clusters with additional contributions from C-H$\cdots$O and lone pair (lp)$\cdots\pi$ interactions, which lead to the overall stability of these clusters.[47] Computational investigations on the structures and bonding in water W_n(n = 1-8)-Bz_m, (m = 1-2) complexes, using an effective fragment potential (EFP) method, have predicted a dominant nature of

H-bonding interactions i.e., O-H···π and C-H···O interactions in all of the larger water-benzene complexes, and benzene is shown to act both as an H-bond donor and acceptor in the water-benzene complexes.[49] The benzene-water interactions are found to be slightly weaker than the water-water interactions, and very small energy differences between different isomers are involved in the formation of such complexes.[49]

The excited state properties of the systems discussed above have received relatively little attention.[56, 57] Recent computational studies on the UV spectroscopy of the cage and the prism conformers of the water hexamer (W_6), and the benzene-bound water hexamer (Bz-W_6) clusters have shown a small red-shift in the main electronic transition of benzene after interacting with the W_6 cluster.[56] It is noticed that benzene influences the water excitations by shifting towards longer wavelengths in both the cage and the prism geometries of Bz–W_6 clusters. Furthermore, in these cluster models, new charge transfer (CT) states are observed. Experimental studies on photo processing of model interstellar ices have revealed three distinct photo-desorption mechanisms in such systems *viz.* (i) direct adsorbate-mediated desorption of benzene, (ii) indirect adsorbate–mediated desorption of water, and (iii) substrate-mediated desorption of both benzene and water.[23] The translational temperature of both desorbed species i.e., the benzene and the water molecules, is found to be higher than the ambient temperature of the complex system. It has been observed experimentally that photon absorption by benzene can make H_2O desorption possible at wavelengths where the photon-absorption cross-section for H_2O is negligible.[22] A recent experimental study on the photodesorption of benzene from H_2O ice has shown a strong dependence of desorption of both Bz and water on the morphology of the ice.[23]

In the experiments discussed above, the photon-stimulated desorption of water from Bz-ice films have been studied at specific wavelengths around 250 nm to represent the interstellar radiation field (ISRF), that corresponds to diffuse regions of molecular clouds in the interstellar medium. However, a computational study of such interstellar ice models can provide deep insight into detailed spectroscopic transitions involved in these processes, and give information about excited states available to the adsorbed benzene. It is evident that a more detailed understanding of the interactions between benzene and the underlying ice surfaces is required. There have been many experimental studies of the adsorption of benzene on both single and polycrystalline metal surfaces.[58-60] To the best of our knowledge, there have been no computational studies in the literature discussing the effects of dangling features of the ice surface on Bz adsorption and UV spectra of Bz-ice complexes. Therefore, the purpose of the present study is two-fold, viz. to both investigate the role of the dangling atoms on Bz adsorption on crystalline water ice, and to investigate the UV spectroscopy and vertical excited states of Bz-ice complexes. Vertical excitation energies and oscillator strengths of the excited states including characterizing the nature of electronic transitions involved in these complexes are the primary focus in this study.

Computational methods and models

Computational methods:

The ONIOM (our Own N-layered Integrated molecular Orbital molecular Mechanics) method[61-64] is one of the most popular hybrid methods. In common practice, ONIOM can be applied to relatively large molecular systems. It produces results of good accuracy at low computational cost. In the ONIOM(QM:MM) formalism, the molecular system is partitioned into two regions; the chemically important partition is treated by a quantum mechanical (QM) method, while the rest of the system is treated by a force-field (MM) method. In a two-layer ONIOM(QM:MM) calculation, the total ONIOM(QM:MM) energy can be obtained as

$$E_{ONIOM}(real) = E_{QM}(model) + E_{MM}(real) - E_{MM}(model) \quad (1)$$

where the model system is treated at both the QM and the MM levels, while the real system is treated at the MM level only. Applications of ONIOM(QM:MM) are many-fold and details are provided in the literature.[65-68] However, the ONIOM(QM:MM) method has not gained much attention in the field of astrochemistry. In this study, we have used the ONIOM(QM:AMOEBA09) method, where we have performed QM calculations with Gaussian09[69] and MM calculations with the Tinker program [70], [71, 72] program.

The AMOEBA (atomic multipole optimized energetics for biomolecular simulation) polarizable force field has been explained in detail in the literature.[73-77] For this potential energy model, the total interaction energy among atoms is expressed as

$$U = U_{bond} + U_{angle} + U_{b\theta} + U_{oop} + U_{torsion} + U_{disp-rep} + U_{elec}^{perm} + U_{elec}^{ind} \quad (2)$$

where the first five terms describe the short-range valence interactions corresponding to the bond stretching, angle bending, bond-angle cross coupling, out-of-plane bending, and torsional rotation, respectively. The last three terms correspond to the non-bonded interactions i.e., dispersion-repulsion (also referred as the vdW interaction), permanent electrostatic, and induced electrostatic contributions. The AMOEBA force-field allows for an accurate description of molecular electrostatic potentials, and errors are shown to reduce by orders of magnitude upon complementing atomic monopoles with dipole and quadrupole moments.[78-80]

AMOEBA includes electronic polarization[74, 76, 81], and treats both intra- and intermolecular polarization consistently *via* Thole's damped interactive induction models.[82] Successful applications of the AMOEBA force-field to study a wide range of properties of gas-phase clusters, liquid water, and ice crystals have been demonstrated in several publications.[73, 74, 83]

In the present work, the geometries of all ice models were optimized with the ONIOM(M06-2X:AMOEBA09) method. We have used a mechanical embedding scheme. The AMOEBA09 atom type definition includes 36 (water O), 37 (water H), 87 (carbon atoms of benzene), and 88 (hydrogen atoms of benzene). The 6-31++G(d,p) basis set [84-87] was used in the QM calculations. In addition, energies of the optimized structures were also obtained by performing single-point energy calculations with ONIOM(LPNO-CCSD:AMOEBA09). The Dunning correlation-consistent[88, 89] cc-pVTZ and cc-pVTZ/C combination basis set was used for the QM calculations. The default cut-off parameters as implemented in the ORCA2.9 program were employed in LPNO-CCSD calculations.[90]

TD-DFT linear response theory[91-94] is one of the popular and most widely used electronic structure methods for calculating vertical electronic excitation energies. Starting from the ONIOM(M06-2X:AMOEBA09) optimized structures, several model structures were generated. TD-DFT calculations on these were performed with the M06-2X[95] functional for all atoms in the model system. Excellent performance of the M06-2X functional for systems involving non-covalent interactions[96, 97], and also electronic excitation energies to valence and Rydberg states have been established previously.[95, 98]

Thus, although there are many possible choices of force-field/density functional combinations, we believe that the ONIOM(M06-2X:AMOEBA09) one is a robust choice to describe both the water and organic molecule subsystems.

ICE MODELS :

Our initial step was to build a few ice cluster models to adsorb benzene and study electronic excitations. For this purpose, two types of models were used, namely A and B. Three water layers are included with a total of 162 H_2O molecules and 156 H_2O molecules, respectively in the A and B models (Figure 1). As the cluster models are large, we have used the ONIOM(M062X:AMOEBA09) approach to optimize them. Then, ONIOM(QM:MM) optimized cluster models were used for the TD-DFT study where all atoms were included in QM.

In model A, the QM region consists of 12 H_2O molecules, and the remaining 150 H_2O molecules are in the MM region. In the case of model B, 8 H_2O molecules are included in the QM region and 148 H_2O molecules are in the MM region. In this study, we focus on four binding sites (two binding sites from model A and another two from B). The binding sites have different dangling features; A1 and B1 (two *d*-H and one *d*-O), and A2 and B2 (one *d*-H and two *d*-O). These binding sites are relevant to the striped phase.[31-33] Depending on the dangling features, four other binding sites can be generated, but those are beyond the scope of the present study.

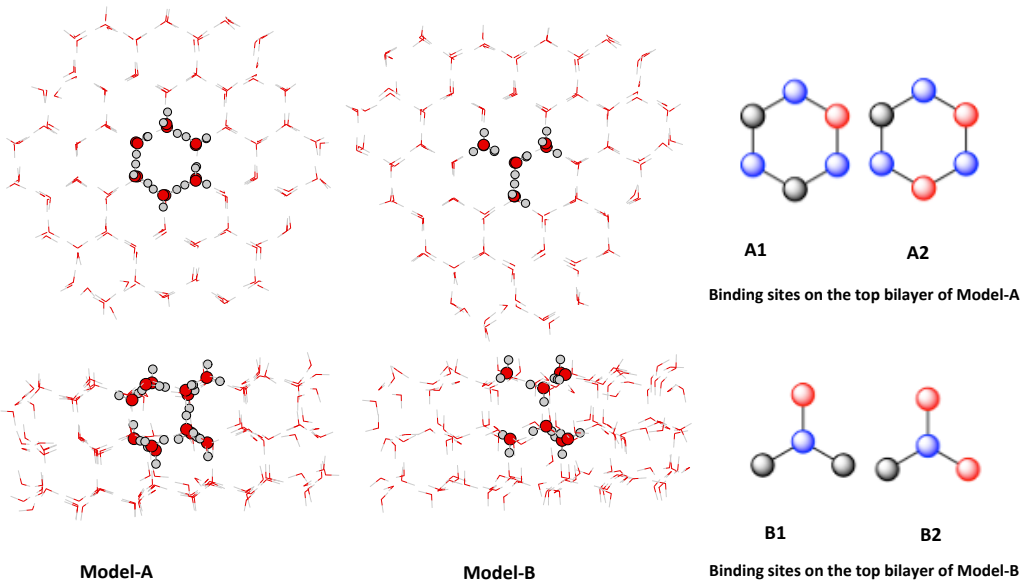

Figure 1. QM/MM structures of model A and B (top and side view to the left), QM/MM structures for A1 and B1 sites are shown here. Illustration of the dangling features at the binding sites to the right. Dangling-hydrogen (*d*-H) and dangling-oxygen (*d*-O) are shown in black circles and red circles, respectively. O atoms in the bilayer immediately below are shown in blue circles.

Results and Discussion

Ground state geometries and energetics of Bz-crystalline ice models:

The ground state geometries of A and B ice models and their respective Bz-ice complexes were fully optimized using the ONIOM(M06-2X:AMOEBA09) approach. The four models with mixed *d*-H and *d*-O dangling bonds were found to bind benzene stronger so in the remainder we focus on these. See Fig S1 (Supporting Information) for the optimized Bz-ice complexes and their total energies.

We have selected the most stable Bz-ice complexes from the A model (i.e., A1, A2) and the B model (i.e., B1, B2). Their key structural parameters are shown in Fig. 2, and calculated binding energies are summarized in Table 1. Binding energies (BE) of the Bz-ice complexes were calculated using the following formula:

$$BE = |(E_{Bz-ice} - (E_{ice} + E_{Bz}))| \quad (3)$$

where E_{Bz-ice}, E_{ice}, and E_{Bz} denote the total energy of the Bz-ice system, crystalline ice I_h, and benzene, respectively.

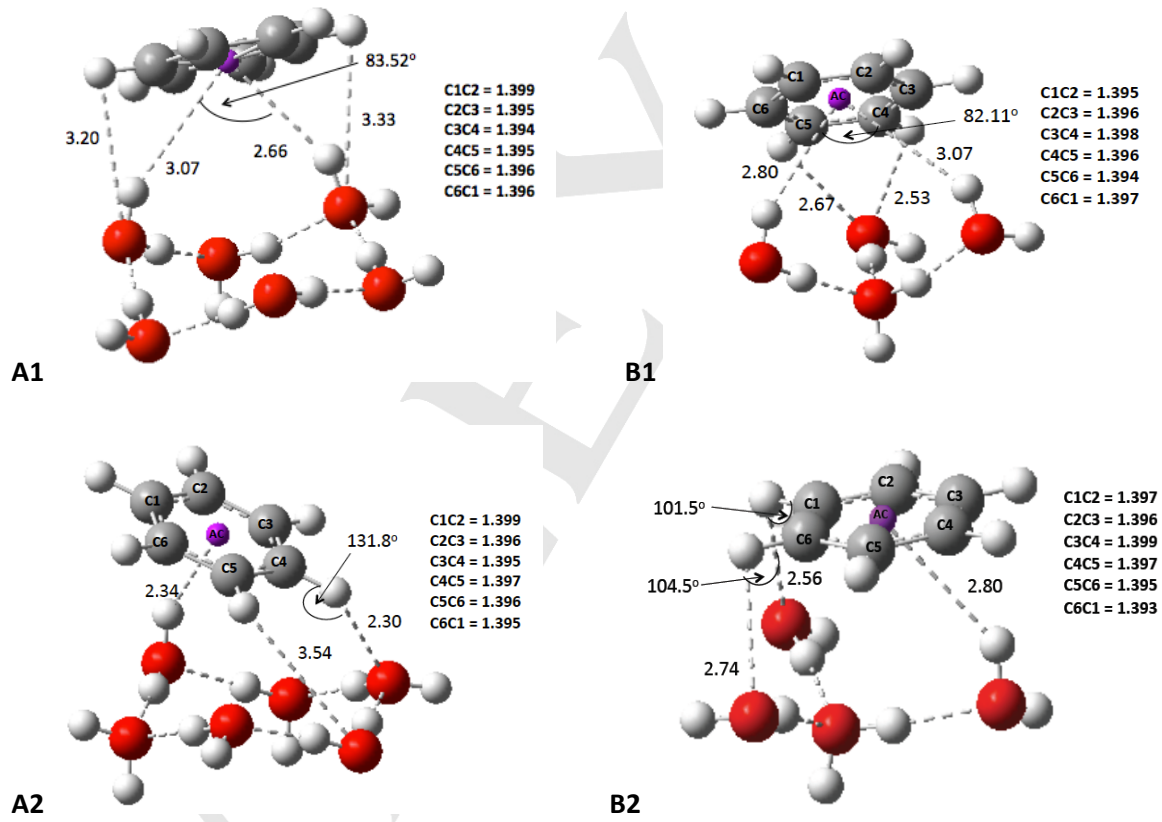

Figure 2. ONIOM(M062X:AMOEBA09) optimized structures of four of the Bz-ice complexes. Only the atoms in the QM region are shown. Carbon-carbon bond lengths in Bz are also given for each binding site. Bond lengths are in Å, bond angles are in degrees, and the aromatic centre of the benzene ring is labelled as AC.

In order to check the effect of the size of the QM region on the benzene binding energies and binding preference, M06-2X single-point calculations were carried out by including all H_2O molecules in the QM region. It is interesting to see that M06-2X binding energies and ONIOM(M06-2X:AMOEBA09) binding energies are in good agreement

(See Table 1 and Fig. 3). Thus, it is evident that the ONIOM(QM:AMOEBA09) method performs quite well on these systems. Also, we have fully optimized A1, B1, and their benzene bound systems by increasing the size of the QM region (48 H_2O molecules in the QM region and 114 H_2O in the MM region). ONIOM(M06-2X:AMOEBA09) optimized structures are shown in Fig. S2 (Supporting Information). The calculated binding energies of each of A1 and B1 are 0.40 eV, and they are in good agreement with M06-2X binding energies. Based on these results, we argue that our ONIOM(QM:MM) model systems provide a good description for benzene binding on ices.

Table 1. Calculated binding energies (in eV) of Bz-ice complexes for geometries optimized at the ONIOM(M06-2X:AMOEBA09) level.

Model	ONIOM (M06-2X:AMOEBA09)	ONIOM (LPNO-CCSD:AMOEBA09)	M06-2X
A1: 2*d*-H 1*d*-O	0.45	0.45	0.43
A2: 2*d*-O 1*d*-H	0.43	0.40	0.41
B1: 2*d*-H 1*d*-O	0.44	0.42	0.43
B2: 2*d*-O 1*d*-H	0.37	0.34	0.36

According to our survey, the calculated binding energies of the four presented Bz bound ice complexes range from 0.37 to 0.45 eV. The largest binding energies were observed for binding sites A1 (0.45 eV) and B1 (0.44 eV). The ONIOM(LPNO-CCSD:AMOEBA09) binding energies are consistent with those of the ONIOM(M06-2X:AMOEBA09) (See Fig. 3), indicating that the dangling features have an effect on the binding energies. Binding of benzene is favoured at the A1 site, where the electron cloud of the benzene interacts with the two *d*-H of the ice surface, which leads to two π····HO type hydrogen bonding interactions. There are two additional C-H···OH hydrogen bonding interactions present in this case, providing more stability thereby giving the highest binding energy for the A1 site. In the case of the A2 site, the binding energy is 0.43 eV. Here two hydrogen atoms of benzene interact with the two *d*-Os of the surface and aromatic centre of benzene interacts with the *d*-H of the surface. This leads to two C-H···OH and one π····HO type hydrogen bonding interactions.

We have performed a similar analysis as above for the B sites. The binding energies of these two sites are 0.44 and 0.37 eV. The binding types are the same as for the A sites and consistent with the results for the A sites. Binding site B1 gives the highest binding energy of the B sites. The π····HO and C-H····O type hydrogen bonding interactions dominate these systems, as has also been seen in previous computational studies.[47, 49]

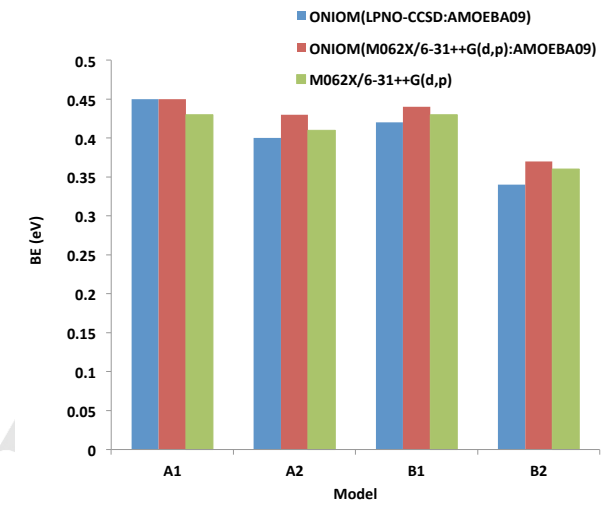

Figure 3. Variation of binding energies (eV) of Bz-I_h complexes versus different levels of theory for all each studied binding site. Note: It is important to mention that the M06-2X/631++G(d,p) calculations were perfomed on the real system, (thus including all atoms in the QM region and leaving no atom in the MM region).

It is important to note that the four binding sites consisting of both *d*-H and *d*-O dangling bonds (A1, A2, B1, and B2) have the characteristics of the 'striped phase'.[33] It has been suggested that an ordered, striped dangling atom pattern is favoured by the ice basal surface as long as the surface remains solid and oxygen-ordered at T $\leq$ 180 K.[33] Thus benzene can strongly adsorb at these sites of crystalline ices at low temperatures.

Electronic excitations in Bz bound ice cluster models:

We have performed TD-DFT calculations on the ONIOM(M06-2X:AMOEBA09) optimized ground state structures of ice cluster models and their respective Bz bound ice clusters. In the TDDFT study, all H_2O molecules in the Bz bound ice clusters were described by the M06-2X functional with the 6-31++G(d,p) basis sets. Ice cluster models of three different sizes for each binding site are taken into account to study the effect of cluster size on electronic excitations in Bz-ice complexes i.e., Bz-$(H_2O)_{12}$; Bz-$(H_2O)_{48}$; Bz-$(H_2O)_{72}$ for binding site A1 and Bz-$(H_2O)_8$; Bz-$(H_2O)_{32}$; Bz-$(H_2O)_{48}$ for binding site B1 (see Fig. 4). Similar calculations are also performed for the binding sites of cluster models A2, and B2.

It should be mentioned that for all of these complexes, we have calculated vertical electronic transitions that are singlet in nature.

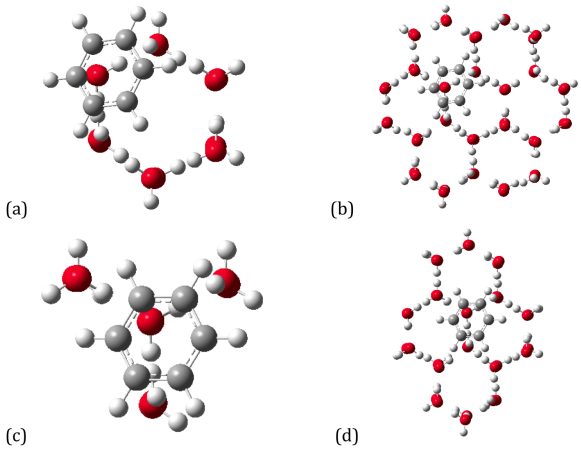

Figure 4. Two of the structures for binding site A1: (a) Bz-$(H_2O)_{12}$; (b) Bz-$(H_2O)_{48}$,and two for binding site B1: (c) Bz-$(H_2O)_8$; (d) Bz-$(H_2O)_{32}$.

ELECTRONIC EXCITATIONS IN MODELS A AND B:

UV spectra obtained by TD-DFT calculations for binding sites A1 and B1 are presented in Fig. 5 and Fig. 6, respectively. In Fig. 7, the corresponding spectra for the A2, and B2 binding sites are shown. We show results for an isolated benzene molecule, a small ice cluster and benzene-ice complexes.

It has been observed experimentally that the UV spectrum of benzene shows absorption bands at 4.9, 6.20, and 6.94 eV related to electronic excitations from the ground state to the excited states with symmetries $^1B_{2U}$, $^1B_{1U}$, and $^1E_{1U}$, respectively.[99] The calculated valence $\pi \rightarrow \pi^*$ excitation energies of Bz (experimental values in parenthesis) are $^1B_{2U}$: 5.59 (4.9[99, 100]), $^1B_{1U}$: 6.39 (6.20[99], 6.19[100]), and $^1E_{1U}$: 7.11 (6.94[99], 6.96[100]) eV. Our results compare well with the experiments for the excitations to the $^1B_{1U}$ and $^1E_{1U}$ excited states, which are computed with an accuracy of about 0.2 eV. The excitation energy of the $^1B_{2U}$ state is however overestimated by about 0.6 eV. It is important to note that the lowest valence transitions of Bz from the ground to the excited states 1^1B_{2U} and 1^1B_{1U} are strictly dipole forbidden on symmetry grounds. The Bz excitation feature at around 174 nm (7.11 eV) is of very high intensity, and corresponds to a dipole allowed electronic transition from the ground to the 1^1E_{1U} excited state.

For Bz-ice complexes, most of the high intensity electronic transitions appear in the range 6.9-7.2 eV. In the case of ice clusters, electronic excitations are strong only at higher energies i.e., above 7.2 eV. It is noticed from the UV spectra that the intensities of the excitation peaks in the Bz-ice complexes for the A1 and A2 sites increase slightly with the size of the ice cluster i.e., as we move from Bz-$(H_2O)_{12}$ to Bz-$(H_2O)_{72}$ (see Fig. 5 and Fig. 7). For binding site A2, strong intensity peaks are centred around 6.95-7.0 eV (178 nm) with only a negligible shift in peak positions with increase in cluster size, while for binding site A1, small shifts in the peak positions are noticed as the cluster size increases from Bz-$(H_2O)_{12}$ to Bz-$(H_2O)_{72}$ and the excitations are seen around 6.93-7.13 eV. Comparing the results for the A1 and A2 binding sites, it is seen that the dangling features of binding site A2 seem to play a smaller role on the UV spectral characteristics than those for the A1 site.

The UV spectral characteristics for cluster model B are similar to those for model A. Also these results show a dependence on the size and the dangling features of the binding site of the ice cluster in Bz-ice complexes (see Fig. 6 and Fig. 7). It is seen that the intensities of the electronic transitions in the Bz-$(H_2O)_{32}$ and Bz-$(H_2O)_{48}$ clusters are slightly stronger than those in the Bz-$(H_2O)_8$ cluster. Rather small shifts in peak positions and their intensities are seen as we move from Bz-$(H_2O)_{32}$ to Bz-$(H_2O)_{48}$ indicating that increasing the size of the ice cluster does not substantially affect the intensities and positions of the electronic transitions.

Next we discuss the nature of the major transitions in the Bz-ice complexes in order to understand the role of Bz and water (W) in generating these strong excitation peaks. Since the binding energies of Bz bound ice clusters are slightly higher for the A1 and B1 binding sites compared to the A2 and B2 sites, as discussed above, we have performed a detailed analysis on the former. We checked the orbital transformations for the excitations that are associated with high oscillator strengths *(f)* or strong intensity peaks in the UV spectra (see Figs. 5 and 6) and the results are presented in Table 2. Additionally, some of the important electronic transitions found in the Bz-$(H_2O)_{12}$ complex for cluster model A2, and Bz-$(H_2O)_8$ complex for cluster model B2 are given in Table 3.

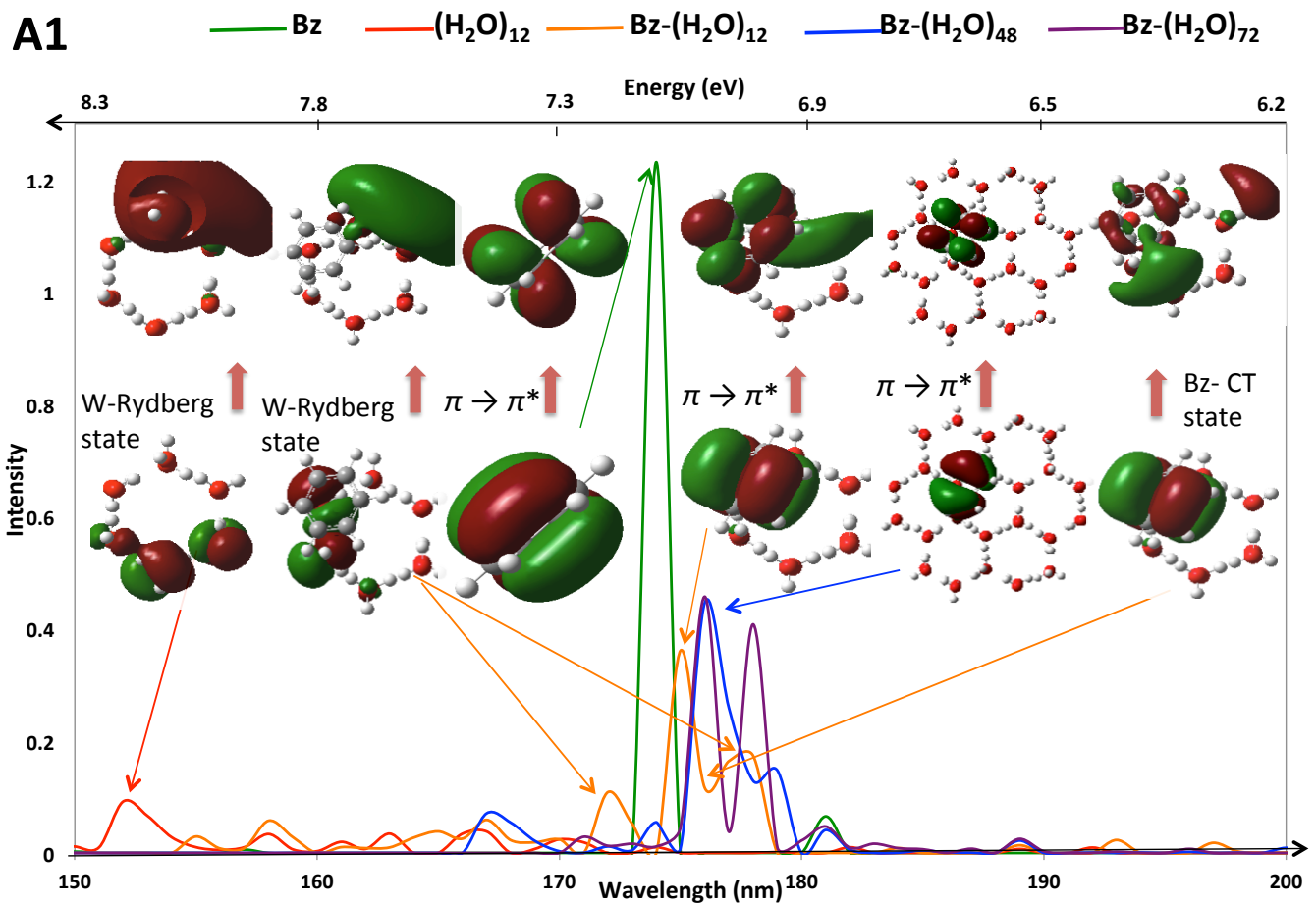

Figure 5. Simulated UV spectra obtained by TD-DFT calculations using the M06-2X hybrid functional and the 6-31++G(d,p) basis set on an isolated Bz molecule and on ONIOM(M062X:AMOEBA09) optimized ground state geometries of cluster model A1. Some key orbitals involved in important electronic transitions are also presented.

In the UV spectra of both the A1: Bz-$(H_2O)_{12}$ and B1: Bz-$(H_2O)_8$ clusters, the two lowest energy vertical $\pi \rightarrow \pi^*$ transitions show small red-shifts (0.05-0.12 eV) compared to isolated Bz. These transitions, i.e. from the ground to the 1^1B_{2U} and 1^1B_{1U} states, which are dipole forbidden in Bz thus become slightly allowed in the Bz-ice complexes *i.e.*,

$$\mathrm{Bz}\,(f = 0.000) \rightarrow \mathrm{A1:Bz} - (\mathrm{H_2O})_{12}(f = 0.004 - 0.018), \mathrm{B1:Bz} - (\mathrm{H_2O})_8(f = 0.001 - 0.005).$$

Similar spectral characteristics are noticed as we increase the size of the ice cluster, and low-lying $\pi \rightarrow \pi^*$ vertical excitations become allowed with nearly the same oscillator strengths for both the A1 and the B1 binding sites, e.g.,

$$(\mathrm{Bz}\,(f = 0.000) \rightarrow \mathrm{A1:Bz} - (\mathrm{H_2O})_{72}(f = 0.002 - 0.005), \mathrm{B1:Bz} - (\mathrm{H_2O})_{32}(f = 0.002 - 0.005).$$

It is found that the strongest transition for the A1: Bz-$(H_2O)_{12}$ complex is at about 7.1 eV (175 nm) and that it is due to a $\pi \rightarrow \pi^*$ electronic transition of benzene. This strong intensity $\pi \rightarrow \pi^*$ electronic transition (bright state) with high oscillator strength is slightly red-shifted with respect to the corresponding dipole allowed transition to the degenerate $^1E_{1U}$ excited states of isolated Bz. The magnitude of the red-shift is about 0.04 eV (~ 1 nm). For the B1: Bz-$(H_2O)_8$ complex, the corresponding transition gives a red-shift of about 0.12 eV (~ 3 nm).

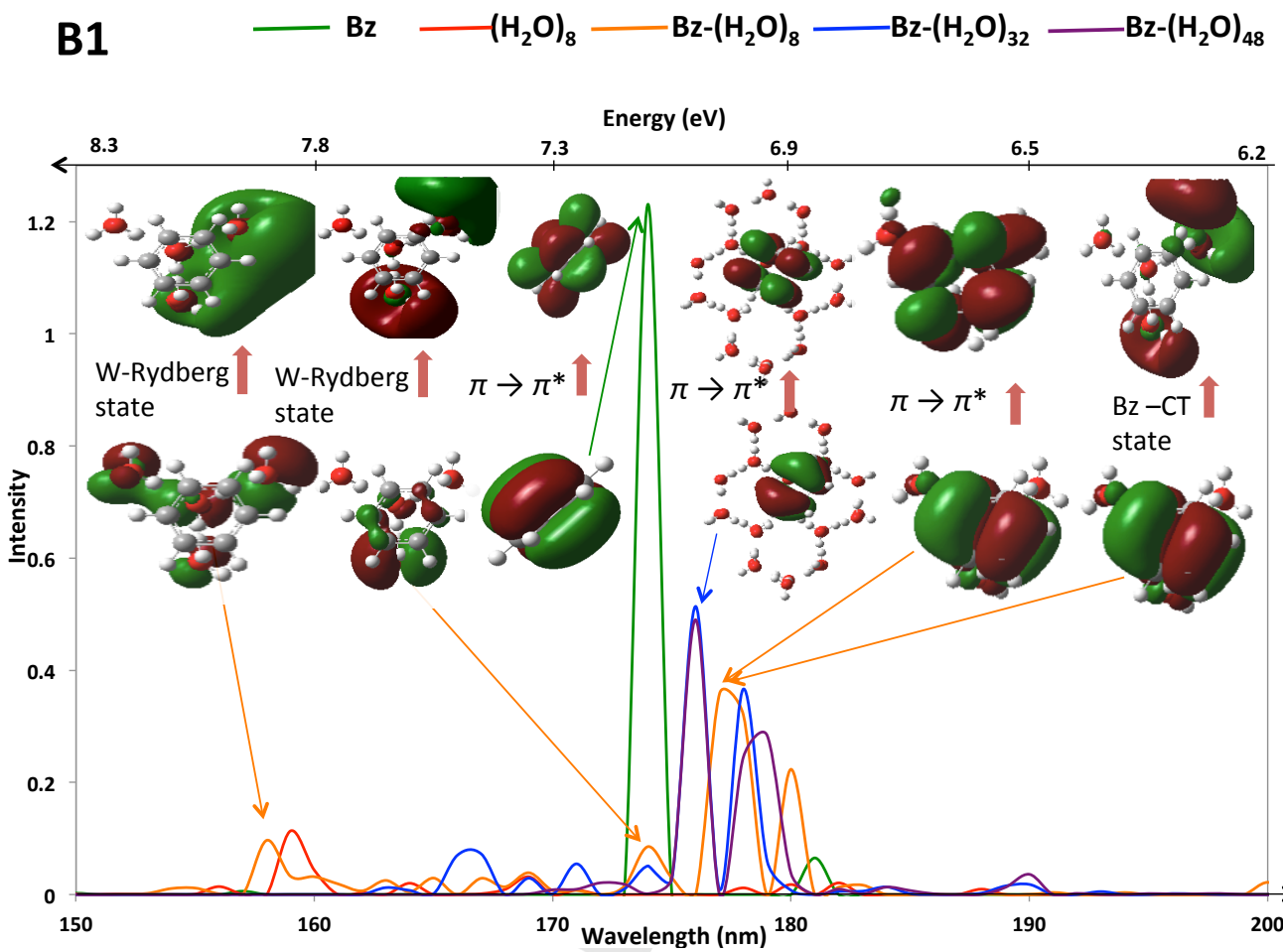

Figure 6. Simulated UV spectra obtained by TD-DFT calculations using the M06-2X hybrid functional and the 6-31++G(d,p) basis set on an isolated Bz molecule and on ONIOM(M062X:AMOEBA09) optimized ground state geometries of cluster model B1. Some key orbitals involved in important electronic transitions are also presented.

The degeneracy of the $^1E_{1U}$ states of Bz is broken by about 0.1 eV (~ 2.5 nm) in A1:Bz-$(H_2O)_{12}$ while it is broken by less than 0.04 eV (< 1 nm) in the B1:Bz-$(H_2O)_8$ complex. The oscillator strengths of these bright $\pi \rightarrow \pi^*$ electronic states are lower in the Bz-ice complexes as compared to isolated Bz, illustrating the effect of the water cluster. Thus it is clear that the spectrum of benzene is changed due to presence of the water cluster.

It is important to note that the highest oscillator strength is found for a $\pi \rightarrow \pi^*$ electronic transition (bright state) in the Bz-$(H_2O)_{72}$ system when compared to the corresponding one in the Bz-$(H_2O)_{12}$ and Bz-$(H_2O)_{48}$ complexes. The electron densities of the key orbitals involved in this main $\pi \rightarrow \pi^*$ electronic transition of Bz remain localized on the benzene ring with increasing ice cluster size. This is consistent with the nature of the orbitals involved in the electronic transition of the isolated Bz molecule. Similar orbital features (*i.e.,* localized electronic densities) are observed in key transitions ($\pi \rightarrow \pi^*$) in both cluster models A and B. It is also evident from our results that both the A and B cluster models are consistent with each other in predicting important electronic transitions in such complex systems.

The existence of close lying Bz charge transfer (CT) states and diffuse states is found in the Bz-ice complexes (see Table 2). These states may influence the water Rydberg type excitations towards longer wavelengths than 170 nm. This has also been seen in recent experimental studies.[22-24] The intensities of water excitations in Bz-ice complexes are also found to be stronger as compared to those in isolated water ice clusters. It is clear from the above results and discussions that

the benzene interactions with the ice clusters are strong enough to affect the UV spectra of Bz-ice complexes.

Table 2. TD-DFT singlet electronic transitions for cluster models A1: Bz-$(H_2O)_{12}$; Bz-$(H_2O)_{48}$; Bz-$(H_2O)_{72}$ and B1: Bz-$(H_2O)_8$; Bz-$(H_2O)_{32}$ (values in parenthesis correspond to singlet $\pi \rightarrow \pi^*$ transition of an isolated benzene molecule).

Model	E (eV)	λ(nm)	Oscillator strength *(f)*	Electronic Transition
A1:	5.54	223.9	0.0038	$\pi \rightarrow \pi^*$
Bz-	(5.59, 4.9[a,b])	(222.0, 253.0[a,b])	(0.0000)	
$(H_2O)_{12}$	6.28	197.4	0.0182	$\pi \rightarrow \pi^*$
	(6.39, 6.20[a,c], 6.19[b])	(194.1,199.9 [a,c], 200.3 [b])	(0.0000)	
	7.07	175.4	0.3606	$\pi \rightarrow \pi^*$
	(7.11, 6.94[a], 6.96[b])	(174.3,178.7[a], 178.1[b])	(0.6158,1.25[d])	
	6.97 (7.11)	177.9 (174.3)	0.1732 (0.6158)	$\pi \rightarrow \pi^*$
	6.99	177.2	0.1415	W-Rydberg state
	7.03	176.4	0.1161	Bz CT state
	7.20	172.3	0.0692	W-Rydberg state
	7.43	166.8	0.0465	W-Rydberg state
A1:	5.53	224.4	0.0046	$\pi \rightarrow \pi^*$
Bz-	6.32	196.3	0.0019	$\pi \rightarrow \pi^*$
$(H_2O)_{48}$	7.05	175.9	0.2550	$\pi \rightarrow \pi^*$
	7.05	175.9	0.1610	W-Rydberg state
	6.99	177.2	0.2068	$\pi \rightarrow \pi^*$
	6.93	178.8	0.1471	Bz CT state
	6.95	178.3	0.1191	Bz CT state
	6.83	181.5	0.0281	$\pi \rightarrow \pi^*$
	7.44	166.7	0.0210	W-Rydberg state
	7.44	166.6	0.0172	$\pi \rightarrow \pi^*$
A1:	5.52	224.4	0.0051	$\pi \rightarrow \pi^*$
Bz-	6.31	196.4	0.0023	$\pi \rightarrow \pi^*$
$(H_2O)_{72}$	7.04	176.1	0.4515	$\pi \rightarrow \pi^*$
	6.97	177.9	0.3945	$\pi \rightarrow \pi^*$
	6.87	180.5	0.0449	Bz CT state
	6.89	180.1	0.0223	Bz CT state
B1:	5.51	224.9	0.0047	$\pi \rightarrow \pi^*$
Bz-$(H_2O)_8$	(5.59, 4.9[a,b])	(222.0, 253.0[a,b])	(0.0000)	
	6.33	196.0	0.0005	$\pi \rightarrow \pi^*$
	(6.39, 6.20[a,c], 6.19[b])	(194.1,199.9 [a,c], 200.3 [b])	(0.0000)	
	6.98	177.5	0.3203	$\pi \rightarrow \pi^*$
	(7.11, 6.94[a], 6.96[b])	(174.3,178.7[a], 178.1[b])	(0.6158, 1.25[d])	
	7.00 (7.11)	177.1 (174.3)	0.2350 (0.6158)	$\pi \rightarrow \pi^*$
	6.87	180.4	0.2234	$\pi \rightarrow \pi^*$
	7.83	158.4	0.0965	W-Rydberg state
	7.14	173.6	0.0855	W CT state
	7.02	176.6	0.1232	Bz CT state
B1:	5.52	224.5	0.0053	$\pi \rightarrow \pi^*$
Bz-	6.32	196.2	0.0018	$\pi \rightarrow \pi^*$
$(H_2O)_{32}$	6.96	178.0	0.3665	$\pi \rightarrow \pi^*$
	7.04	176.3	0.3538	$\pi \rightarrow \pi^*$
	7.03	176.5	0.0656	BZ CT state
	7.04	176.2	0.0579	W-Rydberg state
	7.47	166.0	0.0420	W-CT state
	7.14	173.7	0.0459	Bz CT state
	6.92	179.3	0.0580	Bz CT state

[a]Exptl/Taken from Ref.[99]
[b]Exptl/Taken from Ref.[100]
[c]Exptl/Taken from Ref.[101]
[d]Exptl/Taken from Ref.[102]

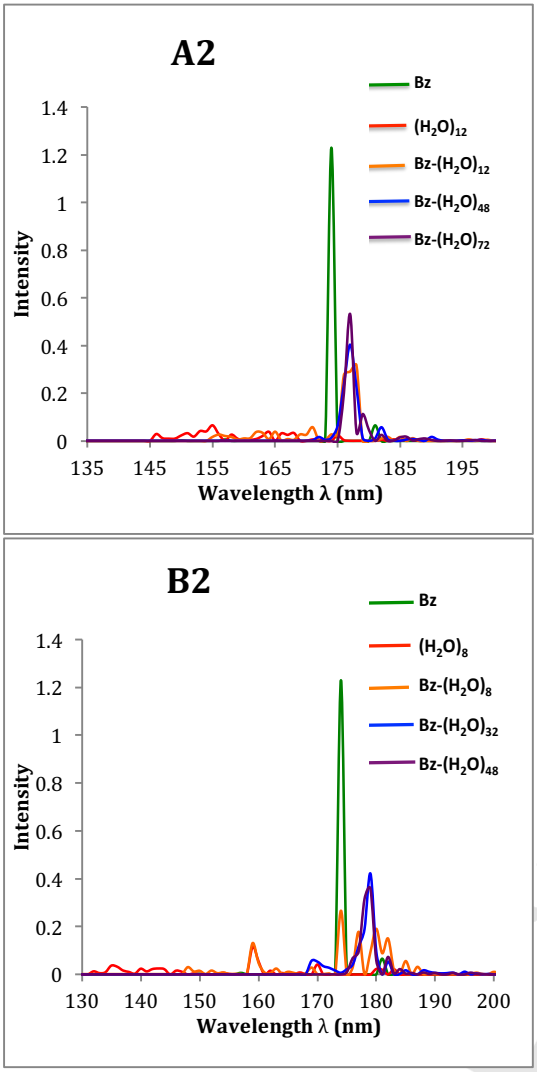

Figure 7. Simulated UV spectra obtained by TD-DFT calculations on an isolated Bz molecule, a small ice cluster and ONIOM(M062X:AMOEBA09) optimized ground state geometries of cluster models A2 and B2.

Table 3. List of important electronic transitions (bright states) obtained by TD-DFT calculations on optimized ground state geometries of Bz-ice complexes for cluster models A2 and B2.

Model	E (eV)	λ(nm)	Oscillator strength *(f)*	Electronic Transition
A2:	7.01	176.9	0.2899	$\pi \rightarrow \pi^*$
Bz-$(H_2O)_{12}$	7.06	175.6	0.2768	$\pi \rightarrow \pi^*$
	6.97	178.0	0.2069	$\pi \rightarrow \pi^*$
	6.95	178.3	0.1102	Bz CT state
B2:	7.01	176.9	0.1781	$\pi \rightarrow \pi^*$
Bz-$(H_2O)_8$	6.83	181.6	0.1500	$\pi \rightarrow \pi^*$
	7.13	173.9	0.1454	$\pi \rightarrow \pi^*$
	7.11	174.4	0.1221	$\pi \rightarrow \pi^*$

Conclusions

We have used the ONIOM(QM:AMOEBA09) method to optimize the benzene-ice complexes. The trends in the ordering of the binding energies of all four ONIOM(M06-2X:AMOEBA09) optimized ground state structures of the studied Bz-ice complexes are in good agreement with our ONIOM(LPNO-CCSD:AMOEBA09) calculations as well as with the M06-2X calculations for the full system, thus predicting good performance of the ONIOM(M06-2X:AMOEBA09) method for modeling benzene-ice complex systems.

We show that hydrogen bonding plays an important role in providing stabilization in benzene-bound ice clusters. The benzene interacts with the ice clusters mainly *via* π····HO and C-H····OH type hydrogen bonding interactions. The binding energies of the benzene-ice complexes depend slightly on the nature of the binding site of the ice surface, with binding sites consisting of two *d*-H and one *d*-O atom providing maximum stabilization to the benzene-ice complexes as compared to binding sites with one *d*-H and two *d*-O atoms. The binding energies of benzene on the four sites of the ice surfaces studied are estimated to be in the range 0.37-0.45 eV.

Our results also show that the UV spectra of benzene-ice clusters show minor differences in peak positions and intensities, depending on the size and nature of the ice surface. They give slightly stronger intensities for excitations as the size of the ice cluster increases. Most of the strong intensity electronic excitations i.e., bright states in the benzene-ice complexes are dominated by benzene. We have also seen some interesting features of benzene-mediated excitations in ice cluster models indicating water excitations at longer wavelengths (> 170 nm) in benzene-ice complexes, predicting the possibility of photon absorption by ice at wavelengths where photon absorption cross-sections are negligible in pure ice, as observed in recent experimental studies.[22, 23] The intensities of ice excitations are also found to increase in benzene-ice complexes relative to those in isolated ice clusters. It is clear that the spectroscopy of benzene is influenced by the presence of the ice cluster, causing red–shifts in the $\pi \rightarrow \pi^*$ electronic transitions of benzene in Bz-ice complexes as compared to those in isolated benzene. The degeneracy of these transitions are broken, but only slightly, compared to the isolated gas-phase benzene. Charge transfer (CT) states and locally excited diffuse states are also important in describing the electronic excitations in the studied benzene-ice complexes. Following this initial application of ONIOM(M06-2X:AMOEBA09) to such a complex system, future work will investigate newer, potentially more accurate, MM models for the water, as well as different density functionals and their combined performance on a wider range of PAHs in ice environments.

Acknowledgements

Thanks are given to Prof. Martin McCoustra for helpful discussions. DS, WMCS, SA, and GN acknowledge the LASSIE

FP7 Marie Curie Initial Training Network (ITN) for funding, while both DS and MJP acknowledge support from the European Research Council (ERC grant number 25899). WMCS acknowledges Prof. Keiji Morokuma (Fukui Institute for Fundamental Chemistry) and Prof. Feliu Maseras (Institute of Chemical Research of Catalonia) for useful discussions..

Keywords: Crystalline ice • Benzene • ONIOM(QM:AMOEBA) • Binding energies • TD-DFT Electronic Excitations

Notes

[a] *Institute of Chemical Sciences, School of Engineering and Physical Sciences, Heriot Watt University, Edinburgh EH14 4AS, United Kingdom.*
[b] *Fukui Institute for Fundamental Chemistry, Kyoto University, Kyoto 606-8103, Japan.*
[c] *University of Gothenburg, Department of Chemistry and Molecular Biology, Kemigården 4, SE-412 96, Gothenburg, Sweden.*
[d] *SINTEF Materials and Chemistry, P.O. Box 4760, NO-7465 Trondheim, Norway.*
**To whom correspondence should be addressed email: m.j.paterson@hw.ac.uk*

Supplementary Information (SI) available: [Ground state structures of all ONIOM(QM:MM) optimized Bz-ice complexes for both models A and B (Fig. S1); ONIOM(QM:MM) optimized structures of Bz-ice complexes for binding site A1 and B1 with larger QM region (Fig. S2), and ONIOM(QM:MM) optimized coordinates of A1 and B1 binding sites.]

References

[1] P. Ehrenfreund, M. A. Sephton *Faraday Discuss.* **2006**, 133, 277-288.
[2] L. J. Allamandola, D. M. Hudgins, C. W. Bauschlicher, S. R. Langhoff *Astron. Astrophys.* **1999**, 352, 659-664.
[3] M. Kassis, J. D. Adams, M. F. Campbell, L. K. Deutsch, J. L. Hora, J. M. Jackson, E. V. Tollestrup *Astrophys. J.* **2006**, 637, 823-837.
[4] H. Kaneda, T. Onaka, I. Sakon *Astrophys. J.* **2005**, 632, L83-L86.
[5] E. Lagadec, O. Chesneau, M. Matsuura, O. De Marco, J. A. D. Pacheco, A. A. Zijlstra, A. Acker, G. C. Clayton, B. Lopez *Astronomy & Astrophysics*. **2006**, 448, 203-212.
[6] L. J. Allamandola, M. P. Bernstein, S. A. Sandford, R. L. Walker *Space. Sci. Rev.* **1999**, 90, 219-232.
[7] W. W. Duley *Faraday Discuss.* **2006**, 133, 415-425.
[8] L. J. Allamandola *Abstr. Pap. Am. Chem. Soc.* **2006**, 231.
[9] L. J. Allamandola, D. M. Hudgins, C. W. Bauschlicher, S. R. Langhoff *Astron. Astrophys.* **1999**, 352, 659-664.
[10] S. A. Sandford, M. P. Bernstein, L. J. Allamandola *Astrophys. J.* **2004**, 607, 346-360.
[11] M. P. Bernstein, S. A. Sandford, L. J. Allamandola *Astrophys. J. Suppl. S.* **2005**, 161, 53-64.
[12] M. P. Bernstein, S. A. Sandford, A. L. Mattioda, L. J. Allamandola *Astrophys. J.* **2007**, 664, 1264-1272.
[13] M. P. Bernstein, S. A. Sandford, L. J. Allamandola, S. Chang, M. A. Scharberg *Astrophys. J.* **1995**, 454, 327-344.
[14] M. P. Bernstein, S. A. Sandford, L. J. Allamandola, J. S. Gillette, S. J. Clemett, R. N. Zare *Science*. **1999**, 283, 1135-1138.
[15] M. S. Gudipati, L. J. Allamandola *Astrophys. J.* **2003**, 596, L195-L198.
[16] M. S. Gudipati, L. J. Allamandola *Astrophys. J.* **2004**, 615, L177-L180.
[17] M. S. Gudipati, L. J. Allamandola *Astrophys. J.* **2006**, 638, 286-292.
[18] C. Dominik, C. Ceccarelli, D. Hollenbach, M. Kaufman *Astrophys. J.* **2005**, 635, L85-L88.
[19] K. Willacy, D. A. Williams *Mon. Not. R. Astron. Soc.* **1993**, 260, 635-642.
[20] J. E. Elsila, M. R. Hammond, M. P. Bernstein, S. A. Sandford, R. N. Zare *Meteorit. Planet. Sci.* **2006**, 41, 785-796.
[21] K. I. Oberg, G. W. Fuchs, Z. Awad, H. J. Fraser, S. Schlemmer, E. F. Van Dishoeck, H. Linnartz *Astrophys. J.* **2007**, 662, L23-L26.
[22] J. D. Thrower, A. G. M. Abdulgalil, M. P. Collings, M. R. S. McCoustra, D. J. Burke, W. A. Brown, A. Dawes, P. J. Holtom, P. Kendall, N. J. Mason, F. Jamme, H. J. Fraser, F. J. M. Rutten *J. Vac. Sci. Technol. A*. **2010**, 28, 799-806.
[23] J. D. Thrower, D. J. Burke, M. P. Collings, A. Dawes, P. D. Holtom, F. Jamme, P. Kendall, W. A. Brown, I. P. Clark, H. J. Fraser, M. R. S. McCoustra, N. J. Mason, A. W. Parker *Astrophys. J.* **2008**, 673, 1233-1239.
[24] J. D. Thrower, M. P. Collings, M. R. S. McCoustra, D. J. Burke, W. A. Brown, A. Dawes, P. D. Holtom, P. Kendall, N. J. Mason, F. Jamme, H. J. Fraser, I. P. Clark, A. W. Parker *J. Vac. Sci. Technol. A*. **2008**, 26, 919-924.
[25] J. Bouwman, H. M. Cuppen, A. Bakker, L. J. Allamandola, H. Linnartz *Astron. Astrophys.* **2010**, 511.
[26] J. Bouwman, H. M. Cuppen, M. Steglich, L. J. Allamandola, H. Linnartz *Astron. Astrophys.* **2011**, 529.
[27] J. Bouwman, D. M. Paardekooper, H. M. Cuppen, H. Linnartz, L. J. Allamandola *Astrophys. J.* **2009**, 700, 56-62.
[28] S. H. Cuylle, L. J. Allamandola, H. Linnartz *Astron. Astrophys.* **2014**, 562.
[29] S. H. Cuylle, E. D. Tenenbaum, J. Bouwman, H. Linnartz, L. J. Allamandola *Mon. Not. R. Astron. Soc.* **2012**, 423, 1825-1830.
[30] J. Cernicharo, A. M. Heras, A. G. G. M. Tielens, J. R. Pardo, F. Herpin, M. Guelin, L. B. F. M. Waters *Astrophys. J.* **2001**, 546, L123-L126.
[31] N. H. Fletcher *Philos. Mag. B*. **1992**, 66, 109-115.
[32] D. Pan, L. M. Liu, G. A. Tribello, B. Slater, A. Michaelides, E. Wang *Phys. Rev. Lett.* **2008**, 101.
[33] V. Buch, H. Groenzin, I. Lit, M. J. Shultz, E. Tosatti *P. Natl. Acad. Sci. USA*. **2008**, 105, 5969-5974.
[34] H. Groenzin, I. Li, V. Buch, M. J. Shultz *J. Chem. Phys.* **2007**, 127.
[35] H. Groenzin, I. Li, M. J. Shultz *Physics and Chemistry of Ice*. **2007**, 191-199.
[36] K. Kim, K. D. Jordan, T. S. Zwier *J. Am. Chem. Soc.* **1994**, 116, 11568-11569.
[37] M. D. Tissandier, S. J. Singer, J. V. Coe *J. Phys. Chem. A*. **2000**, 104, 752-757.
[38] K. Liu, M. G. Brown, C. Carter, R. J. Saykally, J. K. Gregory, D. C. Clary *Nature*. **1996**, 381, 501-503.
[39] S. Maheshwary, N. Patel, N. Sathyamurthy, A. D. Kulkarni, S. R. Gadre *J. Phys. Chem. A*. **2001**, 105, 10525-10537.
[40] D. M. Upadhyay, M. K. Shukla, P. C. Mishra *Int. J Quantum Chem.* **2001**, 81, 90-104.
[41] A. Lenz, L. Ojamae *Phys. Chem. Chem. Phys.* **2005**, 7, 1905-1911.
[42] A. Lenz, L. Ojamae *J. Phys. Chem. A*. **2006**, 110, 13388-13393.
[43] D. M. Bates, G. S. Tschumper *J. Phys. Chem. A*. **2009**, 113, 3555-3559.
[44] Y. Wang, V. Babin, J. M. Bowman, F. Paesani *J. Am. Chem. Soc.* **2012**, 134, 11116-11119.
[45] Y. I. Neela, A. S. Mahadevi, G. N. Sastry *J. Phys. Chem. B*. **2010**, 114, 17162-17171.
[46] A. Lenz, L. Ojamae *Chem. Phys. Lett.* **2006**, 418, 361-367.
[47] M. Prakash, K. G. Samy, V. Subramanian *J. Phys. Chem. A*. **2009**, 113, 13845-13852.
[48] R. N. Pribble, T. S. Zwier *Faraday Discuss.* **1994**, 97, 229-241.
[49] L. V. Slipchenko, M. S. Gordon *J. Phys. Chem. A*. **2009**, 113, 2092-2102.
[50] R. N. Pribble, T. S. Zwier *Science*. **1994**, 265, 75-79.
[51] J. Ma, D. Alfe, A. Michaelides, E. Wang *J. Chem. Phys.* **2009**, 130, 154303.
[52] A. J. Gotch, T. S. Zwier *J. Chem. Phys.* **1992**, 96, 3388-3401.
[53] A. W. Garrett, T. S. Zwier *J. Chem. Phys.* **1992**, 96, 3402-3410.
[54] S. C. Silva, J. P. Devlin *J. Phys. Chem.* **1994**, 98, 10847-10852.
[55] S. Bahr, V. Kempter *J. Chem. Phys.* **2007**, 127, 074707.
[56] D. Sharma, M. J. Paterson *Photochem.Photobiol.Sci.* **2014**, 13, 1549-1560.
[57] D. M. Upadhyay, P. C. Mishra *J. Mol. Struc-TheoChem.* **2002**, 584, 113-133.
[58] P. Jakob, D. Menzel *Surf. Sci.* **1989**, 220, 70-95.
[59] S. Haq, D. A. King *J. Phys. Chem.* **1996**, 100, 16957-16965.
[60] T. J. Rockey, M. C. Yang, H. L. Dai *J. Phys. Chem. B.* **2006**, 110, 19973-19978.
[61] F. Maseras, K. Morokuma *J. Comput. Chem.* **1995**, 16, 1170-1179.
[62] S. Humbel, S. Sieber, K. Morokuma *J. Chem. Phys.* **1996**, 105, 1959-1967.
[63] M. Svensson, S. Humbel, R. D. J. Froese, T. Matsubara, S. Sieber, K. Morokuma *J. Phys. Chem.* **1996**, 100, 19357-19363.
[64] T. Vreven, K. Morokuma *Annu. Rep. Comp. Chem.* **2006**, 2, 35-51.
[65] L. W. Chung, W. M. C. Sameera, R. Ramozzi, A. J. Page, M. Hatanaka, G. P. Petrova, T. V. Harris, X. Li, Z. Ke, F. Liu, H-B. Li, L. Ding and K. Morokuma, *Chem. Rev.* **2015**, 115, 5678-5796.
[66] W. M. C. Sameera, F. Maseras *Phys. Chem. Chem. Phys.* **2011**, 13, 10520-10526.
[67] L. W. Chung, H. Hirao, X. Li, K. Morokuma *WIREs Comput. Mol. Sci.* **2012**, 2, 327-350.
[68] W. M. C. Sameera, F. Maseras *WIREs Comput. Mol. Sci.* **2012**, 2, 375-385.
[69] M. J. Frisch, G. W. Trucks, H. B. Schlegel, G. E. Scuseria, M. A. Robb, J. R. Cheeseman, G. Scalmani, V. Barone, B. Mennucci, G. A. Petersson, H. Nakatsuji, M. L. Caricato, X., H. P. Hratchian, A. F. Izmaylov, J. Bloino, G. Zheng, J. L. Sonnenberg, M. Hada, M. Ehara, K. Toyota, R. Fukuda, J. Hasegawa, M. Ishida, T. Nakajima, Y. Honda, O. Kitao, H. Nakai, T. Vreven, J. A. J. Montgomery, J. E. Peralta, F. Ogliaro, M. Bearpark, J. J. Heyd, E. Brothers, K. N. Kudin, V. N. Staroverov, R. Kobayashi, J. Normand, K. Raghavachari, A. Rendell, J. C. Burant, S. S. Iyengar, J. Tomasi, M. Cossi, N. Rega, M. J. Millam, M. Klene, J. E. Knox, J. B. Cross, V. Bakken, C. Adamo, J.

Jaramillo, R. Gomperts, R. E. Stratmann, O. Yazyev, A. J. Austin, R. P. Cammi, C., J. W. Ochterski, R. L. Martin, K. Morokuma, V. G. Zakrzewski, G. A. Voth, P. Salvador, J. J. Dannenberg, S. Dapprich, A. D. Daniels, Ö. Farkas, J. B. Foresman, J. V. Ortiz, J. Cioslowski, D. J. Fox. **Gaussian 09, Revision D.01, Gaussian Inc., Wallingford CT, 2009.**
[70] I. Rivilla, W. M. C. Sameera, E. Alvarez, M. M. Diaz-Requejo, F. Maseras, P. J. Perez *Dalton Trans.* **2013**, 42, 4132-4138.
[71] J. W. Ponder, F. M. Richards *J. Comput. Chem.* **1987**, 8, 1016-1024.
[72] C. E. Kundrot, J. W. Ponder, F. M. Richards *J. Comput. Chem.* **1991**, 12, 402-409.
[73] P. Y. Ren, J. W. Ponder *J. Phys. Chem. B*. **2003**, 107, 5933-5947.
[74] J. W. Ponder, C. J. Wu, P. Y. Ren, V. S. Pande, J. D. Chodera, M. J. Schnieders, I. Haque, D. L. Mobley, D. S. Lambrecht, R. A. DiStasio, M. Head-Gordon, G. N. I. Clark, M. E. Johnson, T. Head-Gordon *J. Phys. Chem. B*. **2010**, 114, 2549-2564.
[75] Y. Shi, C. J. Wu, J. W. Ponder, P. Y. Ren *J. Comput. Chem.* **2011**, 32, 967-977.
[76] Y. Shi, Z. Xia, J. J. Zhang, R. Best, C. J. Wu, J. W. Ponder, P. Y. Ren *J. Chem. Theory. Comput.* **2013**, 9, 4046-4063.
[77] P. Y. Ren, C. J. Wu, J. W. Ponder *J. Chem. Theory. Comput.* **2011**, 7, 3143-3161.
[78] D. E. Williams *J. Comput. Chem.* **1988**, 9, 745-763.
[79] F. Vignemaeder, P. Claverie *J. Chem. Phys.* **1988**, 88, 4934-4948.
[80] P. N. Day, J. H. Jensen, M. S. Gordon, S. P. Webb, W. J. Stevens, M. Krauss, D. Garmer, H. Basch, D. Cohen *J. Chem. Phys.* **1996**, 105, 1968-1986.
[81] P. Y. Ren, J. W. Ponder *J. Comput. Chem.* **2002**, 23, 1497-1506.
[82] B. T. Thole *Chem. Phys.* **1981**, 59, 341-350.
[83] P. Y. Ren, J. W. Ponder *J. Phys. Chem. B*. **2004**, 108, 13427-13437.
[84] Ditchfie.R, W. J. Hehre, J. A. Pople *J. Chem. Phys.* **1971**, 54, 724-728.
[85] W. J. Hehre, Ditchfie.R, J. A. Pople *J. Chem. Phys.* **1972**, 56, 2257-2261.
[86] Harihara.Pc, J. A. Pople *Theor. Chem. Acc.* **1973**, 28, 213-222.
[87] M. M. Francl, W. J. Pietro, W. J. Hehre, J. S. Binkley, M. S. Gordon, D. J. Defrees, J. A. Pople *J. Chem. Phys.* **1982**, 77, 3654-3665.
[88] D. E. Woon, T. H. Dunning Jr *J. Chem. Phys.* **1994**, 100, 2975-2988.
[89] T. H. Dunning *J. Chem. Phys.* **1989**, 90, 1007-1023.
[90] F. Neese *WIREs Comput. Mol. Sci.* **2012**, 2, 73-78.
[91] E. Runge, E. K. U. Gross *Phys. Rev. Lett.* **1984**, 52, 997-1000.
[92] R. Bauernschmitt, R. Ahlrichs *Chem. Phys. Lett.* **1996**, 256, 454-464.
[93] K. Burke, J. Werschnik, E. K. U. Gross *J. Chem. Phys.* **2005**, 123.
[94] M. A. L. Marques, E. K. U. Gross *Annu. Rev. Phys. Chem.* **2004**, 55, 427-455.
[95] Y. Zhao, D. G. Truhlar *Theor. Chem. Acc.* **2008**, 120, 215-241.
[96] H. R. Leverentz, H. W. Qi, D. G. Truhlar *J. Chem. Theory. Comput.* **2013**, 9, 995-1006.
[97] W. M. C. Sameera, D. A. Pantazis *J. Chem. Theory. Comput.* **2012**, 8, 2630-2645.
[98] Y. Zhao, N. E. Schultz, D. G. Truhlar *J. Chem. Theory. Comput.* **2006**, 2, 364-382.
[99] A. Hiraya, K. Shobatake *J. Chem. Phys.* **1991**, 94, 7700-7706.
[100] E. Pantos, J. Philis, A. Bolovinos *J. Mol. Spectrosc.* **1978**, 72, 36-43.
[101] Lassettr.En, A. Skerbele, M. A. Dillon, K. J. Ross *J. Chem. Phys.* **1968**, 48, 5066-5096.
[102] M. W. Williams, R. A. Macrae, R. N. Hamm, E. T. Arakawa *Phys. Rev. Lett.* **1969**, 22, 1088-1091.

ARTICLE

Benzene–mediated electronic excitations of water towards longer wavelengths (above 170 nm) are noticed in benzene-bound ice clusters, which are however completely absent in isolated water ice clusters as photon absorption cross-section of water is negligible at these wavelengths.

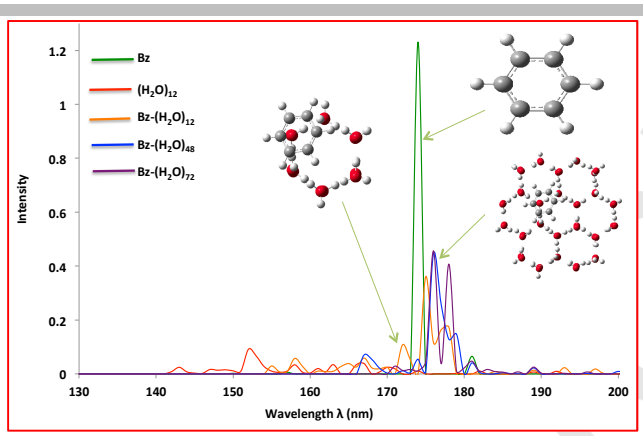

Divya Sharma,[a] W. M. C Sameera,[b,c] Stefan Andersson,[c,d] Gunnar Nyman,[c] and Martin J. Paterson[a]*

Page No. – Page No.

Computational study of the interactions between benzene and crystalline ice I_h: Ground and excited states